Aliphatic polyesters as models for relaxation processes in crystalline polymers: 3. Mechanical relaxation in copolymers of adipic acid with 1,6 and 2,5-hexanediols

R. H. Boyd and P. A. Aylwin
Department of Materials Science and Engineering and Department of Chemical Engineering, University of Utah, Salt Lake City, UT 84112, USA
(Received 25 January 1983; revised 4 April 1983)

The shear moduli of a series of the title polyesters spanning a crystallinity range of 0–60% have been measured as a function of temperature at ≈1 Hz using a torsion pendulum. The experimental isochronal temperature scans of G' and G'' are fitted to phenomenological equations. With only minor adjustments, the same relaxation spectrum parameters as found dielectrically for these polymers (relaxation shape, central relaxation times) fit the mechanical data. Thus, for the β (glass–rubber) relaxation in the amorphous fraction the broadness is very sensitive to the presence of the crystal fraction and becomes increasingly broad as the degree of crystallinity increases. In contrast, the γ process dynamic behaviour is insensitive to the presence of and degree of crystallinity. Unrelaxed and relaxed moduli values are determined for the γ and β processes. A composite model approach is used to determine bounds on the amorphous-phase unrelaxed and relaxed γ and β moduli from the bulk specimen values. As was the case dielectrically, the γ process, in addition to being assigned to the amorphous fraction, has a strength that depends on the diol composition also. The relaxed $(\gamma+\beta)$ amorphous-phase rubbery shear modulus is bound reasonably well from application of the composite model to the bulk specimen values and is assigned the value 100 ± 20 MPa at 250 K. It decreases relatively strongly with increasing temperature.

Keywords Aliphatic polyesters; mechanical relaxation; relaxation strength; relaxation width; amorphous phase modulus; lamellar bounds

INTRODUCTION

The issues and motivation for the present work are explained in the Introduction to Part 2[1]. Again, the effects of the presence of the crystal phase on the relaxation processes in the amorphous fraction is examined. In a completely amorphous uncrosslinked polymer, in passing through the glass transition with increasing temperature, the mechanical modulus (isochronally) decreases precipitously towards a temporary molecular weight dependent rubbery plateau at least several decades in magnitude below the glassy modulus. In a semi-crystalline polymer with a glass transition in the amorphous fraction the re-inforcing effect of the crystals would severely limit the magnitude of this decrease even if no further effects were operative. However, the connections of the amorphous chains to the crystals and even the presence of the crystal surfaces[2] have the potential to modify greatly the mechanical behaviour of the amorphous fraction over that of an unconstrained amorphous phase of the same material. In a sense this is analogous to crosslinking of a rubbery material (and indeed it has been treated as such[3]). The fundamental questions with respect to relaxation are similar to those discussed in Part 2. It would be very desirable to quantify the degree of immobilization of the amorphous fraction by the crystals to establish the extent to which the lack of prominence of the β (glass–rubber) relaxation in certain highly crystalline polymers (LPE, POM) is related to kinetic broadening of the relaxation and to reduction in relaxation strength. In contrast to the dielectric case where the analysis in Part 2 may be the only well-documented case definitely showing that the presence of crystal fraction does indeed reduce the relaxation strength as well as broadening the relaxation, in the mechanical case the amorphous-phase relaxation strength must markedly decrease as this just means that the rubbery amorphous-phase modulus is much higher than for the free amorphous material. It is necessary to establish the magnitude of the amorphous-phase modulus in polymers with a well developed β relaxation and whether it would be reasonable to suppose the relaxed modulus could become so high in highly crystalline polymers as to effectively suppress the β relaxation in an equilibrium sense. The purpose of the present work is to measure the shear modulus of the series of aliphatic polyesters described in Part 2. In a first step phenomenological equations are fitted to the data. Then the interpretation of the relaxed moduli in terms of the separate phase moduli is attempted. To accomplish the latter an adequate composite model for the two-phase mixture is required. Such modelling is inherently more difficult mechanically than dielectrically because the disparity between the phase properties is potentially greater mechanically. However, considerable quantification of the amorphous phase modulus is possible.

0032-3861/84/030340-07$03.00

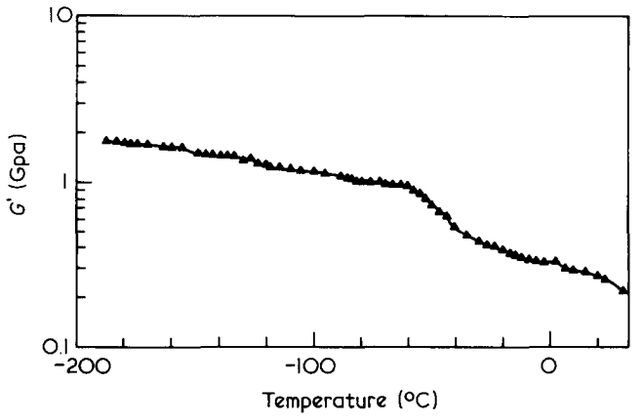

Figure 1 Experimental data for storage shear modulus of semi-crystalline 6–6 homopolymer *versus* temperature (≃1 Hz)

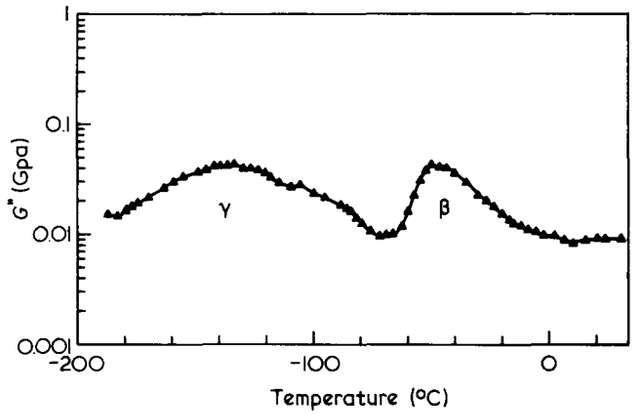

Figure 2 Experimental data for loss shear modulus of 6–6 semi-crystalline homopolymer *versus* temperature (≃1 Hz)

EXPERIMENTAL

The shear modulus was measured approximately isochronally (≈1 Hz) is a free oscillation torsion pendulum. The instrument was designed by E. Baer, J. R. Kastellic and P. A. Hiltner of Case Western University and manufactured for us by the Dycar Corp. It is of the inverted type, with double Dewar jackets. The pendulum is set in motion by an electromagnetic deflector and its excursion is monitored by a light beam reflected from a mirror mounted on the inertia arm and directed onto a photoresistor the output of which is recorded. Temperatures were measured by two thermocouples placed near the specimen and whose outputs were connected to a Fluke digitial thermometer (model 2100A). The measurements were made at constant temperature controlled by a Honeywell model R7350A controller. A nitrogen atmosphere was used in the gas-tight pendulum and liquid nitrogen was used to cool the system to −190°C at the start of an experiment. The storage shear modulus was calculated from[4]:

$$G' = \frac{12\pi^2 IL}{CD^3NP^2}(1+\Lambda/\pi^2) - \frac{CT}{4D^3N} \quad (1)$$

where I is the moment of inertia, L the specimen length, C its width, D its thickness, $P=2\pi/\omega$, (ω the angular frequency), Λ the logarithmic decrement, T the tensile load on the specimen and $N=(1-0.63D/C)$. The decrement was calculated from the successive excursion amplitudes A_i as:

$$\Lambda = \tfrac{1}{2}\ln A_i/A_{i+1} \quad (2)$$

and is related to the loss modulus G'' as:

$$\Lambda = \pi G''/G' \quad (3)$$

The specimens were approximately 50 mm long, 3 mm wide and 0.2 mm thick. They were prepared in a manner similar to the dielectric samples in Part 2. The amorphous 6B–6 specimen ($T_g = -33$°C) was pressed between aluminum foils at room temperature. The sample strip was cut, the pendulum grip loaded and the specimen transferred into the pendulum chamber while immersed in liquid nitrogen.

The samples used are described in Part 2. The mechanical measurements included one more sample than in the dielectric case, a 70–30 specimen; thus 6–6 homopolymer, 90–10, 80–20, 70–30, and 60–40 copolymers and 6B–6 homopolymer were studied.

RESULTS AND DATA FITTING

Experimental results for the extremes of 6–6 crystalline homopolymer and 6B–6 amorphous homopolymer are shown as log G' and log G'' *versus* temperature in *Figures 1–4*. It is necessary to fit the data to phenomenological

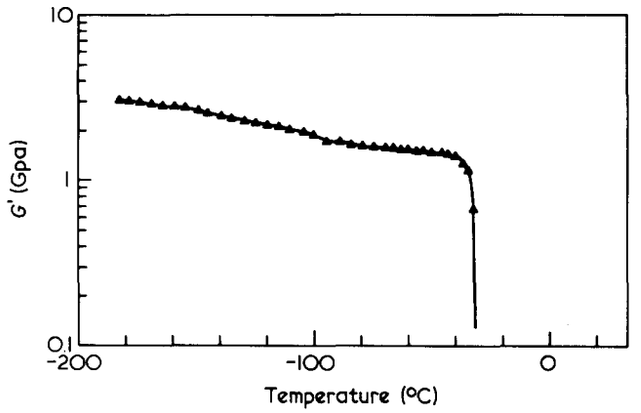

Figure 3 Experimental data for storage shear modulus of amorphous 6B–6 homopolymer *versus* temperature (≃1 Hz)

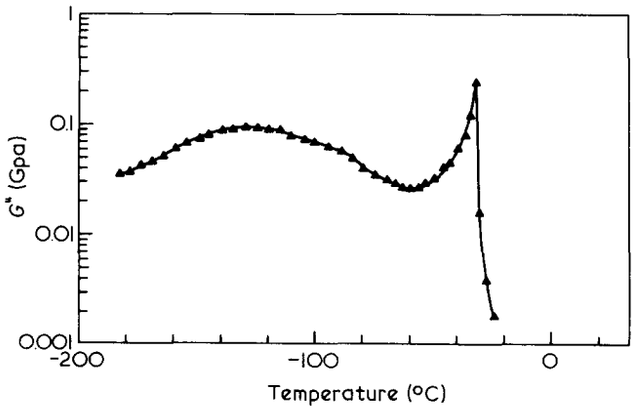

Figure 4 Experimental data for loss shear modulus of amorphous 6B–6 homopolymer *versus* temperature (≃1 Hz)

Table 1 Relaxation spectra for the γ process[a]

	log G_U		log G_R		$\bar{\alpha}$			log τ		
Samples	log G_U^0	$S_U \times 10^3$	log G_R^0	$S_R \times 10^3$	$\bar{\alpha}_0$	$\bar{\alpha}'$	$\bar{\beta}$	A	$-B$	T_∞
6–6	0.29	−0.8	0.02	−0.8	(0.269)	(0.003)	(1.0)	(2514)	(18.87)	0.0
90–10	0.30	−1.0	0.05	−1.0	(0.263)	(0.002)	(1.0)	(2368)	(18.30)	0.0
80–20	0.34	−1.0	0.07	−0.5	(0.261)	(0.002)	(1.0)	(2470)	(18.82)	0.0
70–30	0.35	0.0	0.08	−0.5	0.25	0.002	1.0	2500	18.80	0.0
60–40	0.40	0.0	0.10	0.0	(0.246)	(0.002)	(1.0)	(2732)	(20.20)	0.0
6B–6	0.48	−0.4	0.18	−1.0	(0.226)	(0.001)	(1.0)	(2444)	(17.82)	0.0

[a] Parameters for equation 4 of test. G_U^0 is the unrelaxed modulus at 100 K, S_U is the temperature coefficient of log G_U. G_R^0 is the relaxed γ process modulus at 200 K, S_R is the temperature coefficient of log G_R; $\bar{\alpha}$ is the width parameter at 173 K, $\bar{\alpha}'$ is its temperature coefficient; The skewness parameter $\bar{\beta} = 1$ for all specimens; the temperature dependence of log τ is defined in equation (5). Values in parenthesis were taken unadjusted from *Table 2* of ref. 1

Table 2 Relaxation spectra for the β process[a]

	log G_U		log G_R		$\bar{\alpha}$			log τ		
Sample	log G_U^0	$S_U \times 10^3$	log G_R^0	$S_R \times 10^3$	$\bar{\alpha}^0$	$\bar{\alpha}'$	$\bar{\beta}$	A	$-B$	T_∞
6–6	0.02	−0.8	−0.50	−1.5	(0.132)	(0.002)	(1.0)	(783.0)	(17.76)	(180)
90–10	0.05	−1.0	−0.56	−2.0	(0.176)	(0.003)	(1.0)	(590.3)	(15.00)	186
80–20	0.07	−0.5	−0.60	−3.0	(0.218)	(0.003)	(1.0)	(550.0)	(13.81)	186
70–30	0.08	−0.5	−0.68	−5.0	0.29	0.0025	1.0	756.4	−15.30	176
60–40	0.10	0.0	−0.72	—[b]	0.60	0.0	(1.0)	(802.2)	(15.73)	172
6B–6	0.18	−1.0	see text							

[a] Parameters for equation (4) of text. G_U^0 is the unrelaxed modulus at 200 K (= $G_{R\gamma}^0$), S_U is the temperature coefficient of log G_U^0, G_R^0 is the unrelaxed $\gamma + \beta$ modulus at 260 K, S_R is the temperature coefficient of log G_R^0; $\bar{\alpha}^0$ is the width parameter at 223 K, $\bar{\alpha}'$ is the temperature coefficient; the skewness parameter $\bar{\beta} = 1.0$ for all specimens listed; the temperature dependence of log τ is defined in equation (5). Values in parenthesis were taken from *Table 3* of ref. 1

[b] The temperature interval between complete relaxation of the β process and melting is too small to determine a temperature coefficient

equations to discuss the relaxation broadness and the unrelaxed relaxed moduli. There is, however, a dilemma as the single frequency torsion pendulum data do not provide sufficient information for this purpose. However, it does seem reasonable that the temperature behaviour of the central relaxation times of the dielectric and mechanical relaxation should be similar. Further, the phenomenological equations used in fitting dielectric data should also be fully able to fit mechanical data if properly parameterized. Thus, an attempt was made to fit the mechanical data using the Havriliak–Negami equations[5] (HN) described in Part 2. As the moduli relax to lower values with decreasing frequency a slight modification is necessary and equation (1) of Part 2 is transcribed for the complex shear modulus G^* as:

$$G^* = (G_U - G_R)_1(1-(1+(i\omega\tau_1)^{\bar{\alpha}_1})^{-\bar{\beta}_1}) + (G_U - G_R)_2(1-(1+(i\omega\tau_2)^{\bar{\alpha}_2})^{-\bar{\beta}_2}) + G_{R2} \quad (4)$$

where subscripts R, U refer to the relaxed and unrelaxed values, τ to central relaxation time, $\bar{\alpha}$ to the width parameter, $\bar{\beta}$ to the skewness parameter, ω to angular frequency, and subscripts 1 and 2 to the two relaxation processes ($1 = \gamma$, $2 = \beta$) present.

The aim was to use initially the values of τ, $\bar{\alpha}$ and $\bar{\beta}$ determined from dielectric measurements, selecting only G_R, G_U values specifically for the mechanical measurements, and then to adjust $\bar{\alpha}$, $\bar{\beta}$ values as necessary to preserve the τ values as far as possible between the two types of measurements. This strategy was successful and in the more crystalline samples (6–6 homopolymer and 90–10, 80–20 and 70–30 copolymers) the only adjustments made to the dielectric parameters was to shift the temperature dependence of log τ values for the β process by altering T_∞ slightly in:

$$\log \tau = A/(T - T_\infty) + B \quad (5)$$

and preserving A and B. The $\bar{\alpha}$ values were adapted directly (and $\bar{\beta} = 1$ for these samples). As the 70–30 sample was not measured dielectrically the log τ and $\bar{\alpha}$ values were estimated by interpolation from the dielectric values for the other specimens. For the 60–40 (20% crystallinity) specimen, the β glass–rubber relaxation was sharper mechanically than dielectrically and a higher temperature-independent value of $\bar{\alpha}_2$ was used. For the amorphous 6B–6 homopolymer the torsion pendulum is not suitable for studying the glass transition and only the beginning of the region can be measured. The dielectric $\bar{\alpha}$, $\bar{\beta}$, log τ parameters (Table 3, Part 2) do predict a sharp downturn for log G' at the correct temperature. However, mechanically the beginning of softening appears even sharper than the relaxation of the dielectric constant. The mechanical relaxation spectrum fitting results are shown in *Table 1* for the γ process and in *Table 2* for the β process. A typical fit is shown in *Figures 5* and *6* where log G' and log G'' *versus* temperature calculated from equation (4) and the parameters of *Tables 1* and *2* are compared with the experimental values for the 80–20 copolymer.

The mechanical spectra derived are not necessarily the best possible but it would be difficult to extract more information reliably from isochronal single frequency torsion pendulum scans. In particular the bulk specimen

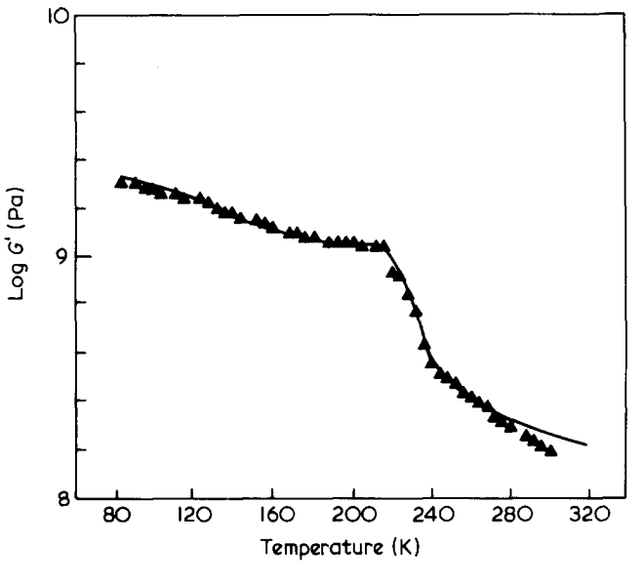

Figure 5 Phenomenological data-fitting. Storage shear modulus of 80–20 copolymer. Points are experimental, curves are calculated using equation (4) of text and parameters of *Tables 1* and *2*

relaxed and unrelaxed modulus values for both the γ and β processes should be reliable. Furthermore, it is evident that the shape and temperature dependence of the dielectric and mechanical processes are remarkably similar. The principal inadequacy of the mechanical fits is the detailed shape of the γ process G'' *versus* T. This is actually an inadequacy of the original dielectric fitting. As discussed in Part 2, dielectrically at the lowest frequency, 10 Hz, the γ process was becoming partially resolved into two processes. However, no attempt was made to accommodate this in the fitting. Mechanically the same thing is apparent but accentuated by even lower frequency (1 Hz). Thus, these fits of the γ log G'' are smoothings of partially-resolved dual processes.

DISCUSSION

As the shape and temperature dependence of both the γ and β mechanical processes are very similar to their dielectric counterparts the discussion of the relaxation dynamics in Part 2 are not repeated. It suffices to reiterate that for the β glass–rubber relaxation in the amorphous fraction the broadness is extremely sensitive to the presence of the crystal fraction and becomes increasingly broad as the degree of crystallinity increases. In contrast, the γ process dynamic behavious process is insensitive to the presence of and degree of crystallinity.

The aim here is to interpret the relaxed specimen moduli in terms of values appropriate to the individual amorphous and crystalline phases. The Voigt uniform strain equation:

$$G=(1-X)G_1+XG_2 \tag{6a}$$

and the Ruess uniform stress equation:

$$1/G=(1-X)/G_1+X/G_2 \tag{6b}$$

where 1, 2 refer to the amorphous and crystal phases, respectively, and X is the degree of crystallinity, are upper and lower bounds, respectively, on G. However, these bounds are very poor if G_1 and G_2 differ greatly. Other approaches for composite mixtures have been discussed previously[6,7] and the reader is referred to these discussions for a fuller account of the literature. Here, an improved approach is used which has been developed recently[7]. It is the mechanical counterpart of the bounding method for the dielectric constant of lamellar structures used in Part 2. The details are more complicated mechanically than dielectrically. The resulting equations used here for the upper and lower bounds to the shear modulus, G(upper) and G(lower), of a macroscopically isotropic crystalline composite with locally lamellar structure are enumerated in the Appendix.

The inputs for the calculation of G(upper) and G(lower) are the elastic constant array for the amorphous fraction (which when assumed to be isotropic requires two independent constants; a shear modulus G_1 and a Poissons ratio ν, for example) and the elastic constant array for the crystal fraction, C_2. For the orthotropic symmetry that seems appropriate for lamellar structures and for many polymer crystals also, nine elastic constants are required. The Poissons ratio for the amorphous fraction is regarded as a fixed parameter with a value of 0.33. The shear modulus G_1 of the amorphous fraction is the quantity the value for which needs to be inferred from the experimental data. The elastic constants of the polyester crystal are not known but they should be similar to those for the structurally similar polyethylene. As an expedient the C_2 array used for polyethylene[7] was adapted by multiplying the elastic constants by a single multiplier to be regarded as an adjustable parameter (F_C).

In *Figure 7* the experimental values of the unrelaxed modulus (at 100 K), the relaxed γ process modulus = unrelaxed β process modulus (at 200 K), and the relaxed $\gamma+\beta$ modulus (at 250 and 300 K) are plotted *versus* the degree of crystallinity for each of the six specimens, the values being taken from *Tables 1* and *2*. First an attempt to

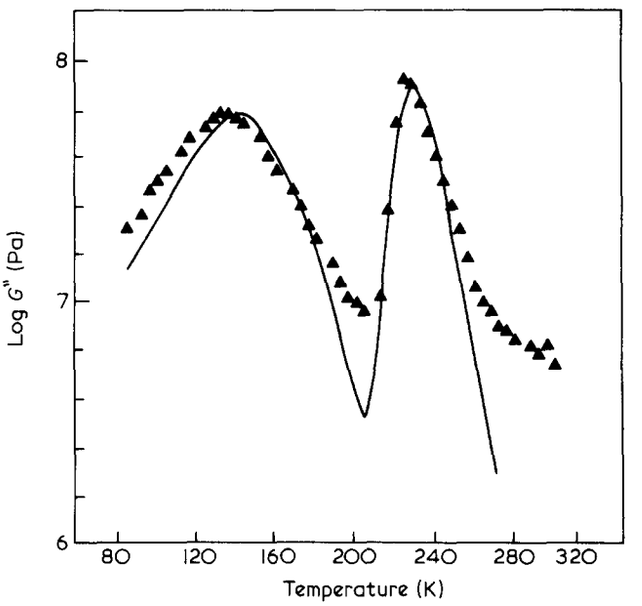

Figure 6 Phenomenological data-fitting. Loss shear modulus of 80–20 copolymer. Points are experimental, curves are calculated using equation (4) of text and parameters of *Tables 1* and *2*

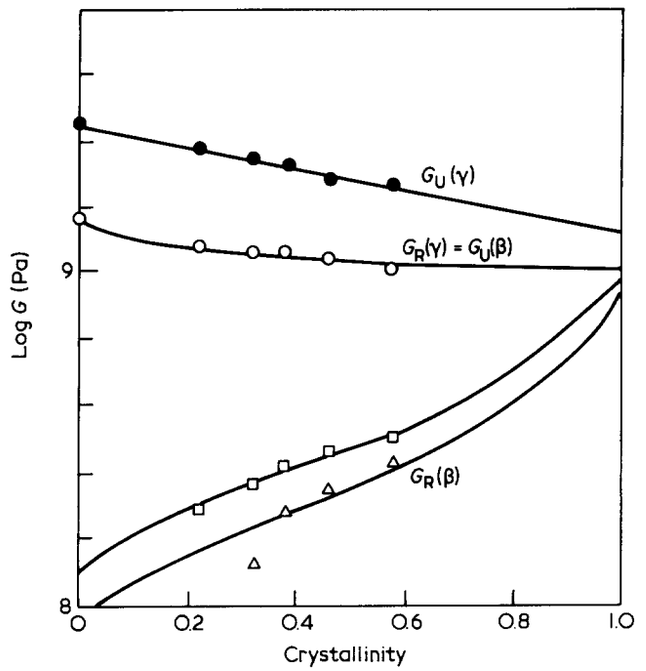

Figure 7 Relaxation strength *versus* crystallinity. Lower bound composite fits. Unrelaxed and relaxed shear moduli for γ and β processes *versus* crystallinity. Points are derived experimental ones (from *Tables 1* and *2*). (●, unrelaxed γ process modulus, 100K; ○, relaxed γ, unrelaxed β modulus, 200K; □, △, relaxed $\gamma+\beta$ process modulus at 250, 300K, respectively). Curves are calculated fits using lower bound lamellar composite equations. Relaxed γ process G_R^γ curve (200K) uses equation (8) of the text for G_1 and assumed the γ process occurs only in amorphous fraction and that 6–6 units contribute 2.1 times the strength of the 6B–6 units. See text for amorphous-phase shear modulus values G_1 used at each temperature in composite equation to calculate curves

lower bound equations (G)lower), Appendix) was made as follows. At the lowest temperature (glassy amorphous phase plus crystals, 100 K) a single crystallinity independent value of G_1 and the crystal-phase elastic constant multiplier, F_C, were adjusted to attempt to fit the experimental points. The result for $G_1 = 2.9$ GPa, $F_C = 0.40$ in the lower bound equation is shown as the curve at 100 K in *Figure 7*.

For the next curve, the relaxed γ process values (200 K), the procedure used for the dielectric strength is followed; i.e. it is assumed that the process occurs only in the amorphous fraction but that the 6–6 and 6B–6 units contribute differently to the relaxed modulus. The site theory[8,9] of mechanical relaxation invokes additivity of compliance contributions so that for the relaxed γ process amorphous phase shear modulus G_1:

$$1/G_1 = \bar{n}_1^A \bar{S}_B + \bar{n}_1^B \bar{S}_B + 1/G_{1U} \qquad (7)$$

where $\bar{n}_1^A$, $\bar{n}_1^B$ are the concentrations of A (=66–6) and B (=6B–6) units, respectively, in the amorphous phase, $\bar{S}_B$, $\bar{S}_B$ are the compliance strengths contributed by these units and G_{1U} is the unrelaxed amorphous phase modulus. By analogy with equation (3) of Part 2, this is rewritten as:

$$1/G_1 = 1/G_{1U} + \bar{N}\bar{S}_A(1-X-P_B)/(1-X) + \bar{N}\bar{S}_B P_B/(1-X) \qquad (8)$$

where $\bar{N}$ is the total sample concentration of A and B units, P_B is the mol fraction of B units in the specimen, and X is the degree of crystallinity. Both G_{1U} and F_C at 200 K were taken as the values determined at 100 K but corrected for the effects of thermal expansion as $G_{1U} = 2.9 \times 10^\delta$ and $F_C = 0.40 \times 10^\delta$ where $\delta = -1.0 \times 10^{-3}(T - 100\ \text{K})$. The temperature coefficient is consistent with results for polyethylene[6,7]. Thus, $G_{1U} = 2.4$ GPa along with $\bar{N}\bar{S}_A = 0.53$, $\bar{N}\bar{S}_B = 0.25$ give values of G_1 from equation (8) that inserted in the lower bound composite equation in turn give the calculated curve (at 200 K) in *Figure 7*.

For the next two curves, the relaxed $\gamma+\beta$ moduli (at 250 K and 300 K), an attempt is made to establish whether the same degree of crystallinity independent value of G_1 can be used to fit all of the specimens at each temperature. This may well be reasonable as in the dielectric case although the presence of the crystal phase reduces the dielectric relaxation strength (and the correlation factor g) of the amorphous $\gamma+\beta$ process the variation of $\gamma+\beta$ correlation factor among the various crystalline specimens is minor (Figure 14 in Part 2). Curves calculated using $G_1 = 0.13$ GPa at 250 K and 0.090 GPa at 300 K are shown in *Figure 7*.

Figure 7 shows that the lower bound lamellar composite equation represents reasonably accurately the shear modulus behaviour. To fit the upper bound relations (G(upper), Appendix) to the data the crystal phase properties are assumed to be fixed and the same values of F_C as in the lower bound fittings are used. *Figure 8* shows the fits achieved using the same parameters at 100 K for the unrelaxed shear modulus and at 200 K for the relaxed γ process modulus as used in the lower bound fit (*Figure 7*) but using $G_1 = 0.08$ GPa at 250 K and $G_1 = 0.035$ GPa at 300 K for the relaxed amorphous phase $\gamma+\beta$ modulus. It is evident that the fits are not as good as

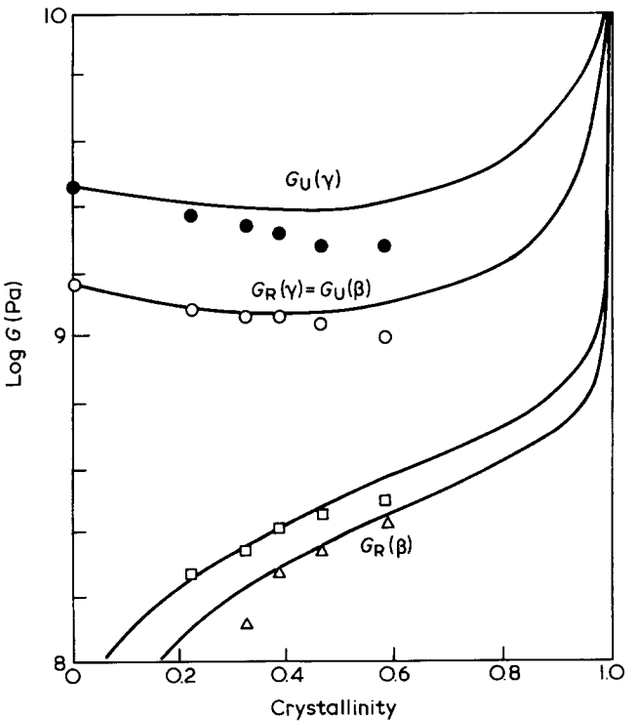

Figure 8 Upper bound composite fits. Same details as *Figure 7* except upper bound lamellar composite equations were used and different values of amorphous-phase shear modulus, G_1, at 250K, 300K were selected (see text for values)

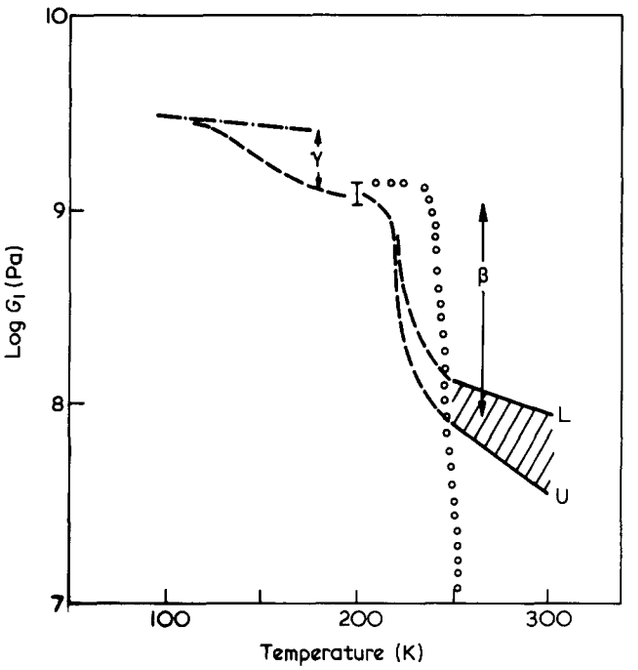

Figure 9 The modulus of the amorphous phase. Unrelaxed and relaxed amorphous fraction shear modulus, G_1, for γ and β processes. For the γ process the same values are inferred from lower and upper bound fits for G_1 (unrelaxed) (—·—·—) and G_1 (relaxed) (I, see text for explanation of vertical bar) (but lower bound fit is better). For the relaxed $\gamma+\beta$ processes (250→300K) bounds on G_1 from both lower (L) and upper bound (U) equations are shown and intermediate values are in shaded area. Dashed lines (– – –) are schematic of relaxation between unrelaxed, relaxed values for γ and β processes (at ≃1 Hz). Open circle curve (○) represents actual behaviour of 6B–6 amorphous homopolymer and the chain segments of which are unconstrained by a crystal phase

Most interestingly, it is evident that the relaxed amorphous $\gamma+\beta$ modulus in *Figure 9* is reasonably well specified by the bounds. $\dot{G}=100\pm20$ MPa at 250 K and decrease relatively rapidly with increasing temperature. This value is believed to be the most reliable estimate of the amorphous fraction relaxed rubbery modulus in a semi-crystalline polymer yet available. Clearly, 100 MPa is an extremely high shear modulus for a material to be regarded as rubbery. To contrast this very high relaxed amorphous-phase modulus in the crystalline samples *Figure 9* also shows the actual behaviour of G' of the 6B–6 amorphous homopolymer the chain segments of which are not confined by the crystal phase.

Finally, returning briefly to the fitting of the composite equations to the moduli it is apparent that at low temperature (100 K) unrelaxed experimental moduli plotted against crystallinity show the specimen G to *decrease* with increasing crystallinity. This is surprising and could be the result of several factors. In the lower bound fit of *Figure 7* the effect is accomodated simply by invoking a crystal elastic constant matrix that leads to an isotropic aggregage average for the 100% crystalline phase (right-hand extreme) that is lower than the amorphous modulus G_1 (left-hand, zero crystallinity extreme in the plot). However, the same crystal elastic constant matrix used in the upper bound composite equations leads to an aggregate average 100% crystalline phase value that is many times higher than G. So the real situation may perhaps be intermediate, the 100% crystalline aggregate having a shear modulus higher than the amorphous phase but with a minimum in the plots at intermediate crystallinity as a composite effect in mixing highly anisotropic crystals with the isotropic amorphous phase. As an illustration a Halpin–Tsai[10]-form equation

for the lower bound lamellar composite equations. Slightly better fits at 100 K for the unrelaxed modulus and 200 K for the relaxed γ process modulus (but not as good as the fit in *Figure 7*) could be obtained by lowering F_C (to ≈0.2) but this does not allow the crystal properties to be known and fixed in both lower and upper bound fitting. Conversely, lowering the F_C value used in the lower bound fitting (*Figure 7*) would give poorer fits; thus, the higher value of $F_C=0.4$ as likely to be more realistic.

Considering this approach of lower and upper bound lamellar composite fitting, it is concluded that of the two extremes, the lower bound behaviour gives a better overall representation, espectially for the low-temperature behaviour in the unrelaxed (100 K) moduli and relaxed γ process (200 K) moduli. More importantly, both extremes give a reasonable representation of the relaxed $\gamma+\beta$ modulus; especially at 250 K. At 300 K the experimental moduli turn down faster at low crystallinity than the composite equations predict for the degree of crystallinity independent G_1. For the higher crystallinity specimens particularly, it is reasonable to regard the lower bound fitting in *Figure 7* and the upper bound fitting in *Figure 8* as providing upper and lower bounds, respectively, on the amorphous-phase shear modulus G_1. These resulting bounds on G_1 are plotted in *Figure 9*. The vertical bar for the relaxed γ process amorphous shear modulus at 200 K shows the range of G_1 indicated by equation (8) for the 6–6 homopolymer ($P_B=0$) to the 6B–6 homopolymer ($P_B=1$).

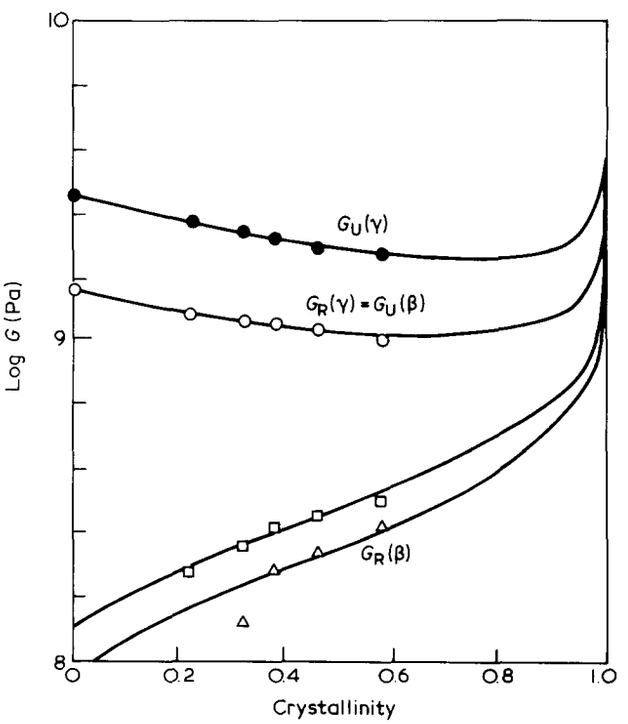

Figure 10 Intermediate fit (between lower and upper bound equations) to unrelaxed and relaxed γ and β process moduli (ξ in equation (9) = 0.1). The fit is similar to that in *Figure 7* but upturn to higher values of shear modulus at 100% crystallinity is evident

is used as an interpolating function between lower and upper bound behaviour; thus:

$$G=(1+\xi G(\text{upper}))/(\xi+1/G(\text{lower})) \quad (9)$$

For $\xi\to 0$ this reduces to G(lower) and for $\xi\to\infty$ to G(upper). In *Figure 10* calculated curves are shown of G *versus* crystallinity with the same input parameters as used in the *Figure 7* lower bound fits inserted into both G(lower) and G(upper) and for a value of $\xi=0.1$. It is evident that the fit of *Figure 7* is essentially undisturbed. Only an upturn of G at very high crystallinity is introduced, one sufficient to accomodate the 100% crystalline aggregate having a higher shear modulus than the completely amorphous opposite extreme. This feature of $\xi=0.1$ would then of course be entirely consistent with any conclusion represented by *Figure 9*. Another possibility which sould be mentioned is that the amorphous-phase modulus could be dependent on chemical composition in the glassy unrelaxed state (100 K) as well as in the relaxed state above the γ process (200 K). Therefore, equation (8) (with different values of $\bar{S}_A, \bar{S}_B$) should perhaps be used at 100 K for the unrelaxed amorphous modulus also. In trials good fits but not as good as those in *Figure 7* were obtained at 100 and 200 K using this approach. Higher values of the crystal elastic constant multiplier ($F_C=0.66$) also resulted. More importantly, the values of G_1 for the relaxed $\gamma+\beta$ process (250, 300 K) from the lower and upper bound fits are essentially unchanged by this refinement.

ACKNOWLEDGEMENT

The authors are indebted to the National Science Foundation, Division of Materials Research, Polymers Program (DMR 80 18326) for financial support of this work.

REFERENCES

1 Boyd, R. H. and Aylwin, P. A. *Polymer* 1984, **25**, 330
2 Lohse, D. J. and Gaylord, R. J. *Polym. Eng. Sci.* 1978, **18**, 513
3 Krigbaum, W. R., Roe, R. J. and Smith, K. J. *Polymer* 1964, **5**, 533
4 Inoue, Y. and Kobatake, Y. *Kolloid Z.* 1958, **159**, 18
5 Havriliak, S. and Negami, S. *Polymer* 1967, **8**, 161
6 Boyd, R. H. *Polym. Eng. Sci.* 1979, **19**, 1010
7 Boyd, R. H. *J. Polym. Sci., Polym. Phys. Edn.* 1983, **21**, 493
8 Zener, C. 'Elasticity and Anelasticity of Metals' University of Chicago Press, Chicago, IL, 1948
9 Huntington, H. B. and Johnson, R. A. *Acta Met.* 1962, **10**, 281
10 Tsai, S. W., Halpin, J. C. and Pagano, N. J. 'Composite Materials Work-shop' Technomic, Stamford, CT, 1968

APPENDIX

The elastic constant matrix of the crystal phase, 2, assumed to have orthorhombic or higher symmetry is:

$$C_2=\begin{bmatrix} C_{11}(2) & C_{12}(2) & C_{13}(2) & 0 & 0 & 0 \\ C_{12}(2) & C_{22}(2) & C_{23}(2) & 0 & 0 & 0 \\ C_{13}(2) & C_{23}(2) & C_{33}(2) & 0 & 0 & 0 \\ 0 & 0 & 0 & C_{44}(2) & 0 & 0 \\ 0 & 0 & 0 & 0 & C_{55}(2) & 0 \\ 0 & 0 & 0 & 0 & 0 & C_{66}(2) \end{bmatrix}$$

its inverse $S_2=C_2^{-1}$ has the same structure but with elements $S_{11}(2)$, $S_{12}(2)$, etc. If the amorphous phase, 1, is assumed to be isotropic its elastic constant matrix C_1 simplifies to $C_{11}(1)=C_{22}(1)=C_{33}(1)=\lambda+2G_1$ where $\lambda=2\nu_1 G_1/(1-2\nu_1)$, $C_{12}(1)=C_{13}(1)=C_{23}(1)=\lambda$, and $C_{44}(1)=C_{55}(1)=C_{66}(1)=G_1$. The inverse $S_1=C_1^{-1}$ has elements $S_{11}(1)$, $S_{12}(1)$, etc. The elastic constant array C of the lamellar composite consisting of extended alternating thin layers of amorphous and crystalline phases and its inverse $S=C^{-1}$ are written in terms of the elements of C_1, S_1, C_2 and S_2 and the volume fractions of the amorphous and crystalline phases X_1 and X_2 as[7]:

$$C_{11}=X_1C_{11}(1)+X_2C_{11}(2)$$
$$C_{12}=X_1C_{12}(1)+X_2C_{12}(2)$$
$$C_{22}=X_1C_{22}(1)+X_1C_{22}(2)$$
$$C_{33}=(S_{11}S_{22}-S_{12}^2)/DS$$
$$C_{13}=(S_{12}S_{23}-S_{22}S_{13})/DS$$
$$C_{23}=(S_{13}S_{12}-S_{11}S_{23})/DS$$
$$C_{44}=1/S_{44},\ C_{55}=1/S_{55}$$
$$C_{66}=1/S_{66}=X_1C_{66}(1)+X_2C_{66}(2)$$

and where:

$$S_{13}=X_1S_{13}(1)+X_2S_{13}(2)$$
$$S_{23}=X_1S_{23}(1)+X_2S_{23}(2)$$
$$S_{33}=X_1S_{33}(1)+X_2S_{33}(2)$$
$$D=C_{11}C_{22}-C_{12}^2$$
$$S_{11}=C_{11}/D+S_{13}^2/S_{33}$$
$$S_{12}=-C_{12}/D+S_{13}S_{23}/S_{33}$$
$$S_{22}=C_{11}/D+S_{23}^2/S_{33}$$
$$S_{44}=X_1S_{44}(1)+X_2S_{44}(2)$$
$$S_{55}=X_1S_{55}(1)+X_2S_{55}(2)$$
$$DS=S_{33}/(C_{11}C_{22}-C_{12}^2)$$

The matrix C with elements C_{11}, C_{12}, etc. above when spatially averaged to $\langle C\rangle$ for a randomly oriented material has elements:

$$A_{11}=A_{22}=A_{33}=(3A+2B+4C)/5$$
$$A_{12}=A_{13}=A_{23}=(A+4B-2C)/5$$
$$A_{44}=A_{55}=A_{66}=(A-B+3C)/5$$

where $A=(C_{11}+C_{22}+C_{33})/3$, $B=(C_{12}+C_{13}+C_{23})/3$, and $C=(C_{44}+C_{55}+C_{66})/3$. The upper bound to the shear modulus of this isotropic material is:

$$G(\text{upper})=A_{44}$$

When the matrix S (with elements S_{11}, S_{12}, etc.) is spatially averaged to $\langle S\rangle$ for a randomly-oriented material, the elements are:

$$A'_{11}=A'_{22}=A'_{33}=(3A'+2B'+4C')/5$$
$$A'_{12}=A'_{13}=A'_{23}=(A'+4B'-2C')/5$$
$$A'_{44}=A'_{55}=A'_{66}=(A'-B'+3C')/5$$

where $A'=(S_{11}+S_{22}+S_{33})/3$, $B'=(S_{12}+S_{13}+S_{23})/3$ and $C'=(S_{44}+S_{55}+S_{66})/12$. The lower bound to the shear modulus is:

$$G(\textit{lower})=1/(4A'_{44})$$